

# MAGNETIC CONTRIBUTION TO THE SPECIFIC HEAT OF $\text{Pb}_{1-x}\text{Eu}_x\text{Te}$

M. Górska, A. Łusakowski, A. Jędrzejczak, Z. Gołacki, and R.R. Gałazka  
*Institute of Physics, Polish Academy of Sciences, Al. Lotników 32/46, 02-668 Warsaw, Poland*

J.R. Anderson and H. Balci\*  
*Department of Physics, University of Maryland, College Park, MD 20742*

The temperature dependence of the magnetic specific heat has been studied experimentally and theoretically in the semimagnetic semiconductor  $\text{Pb}_{1-x}\text{Eu}_x\text{Te}$  for  $x=0.027$  and  $x=0.073$ , over the temperature range from 0.5 K to 10 K, in magnetic fields up to 2 T. There was a maximum in the magnetic specific heat between 1 and 3 K even in zero and low magnetic fields; this maximum shifted toward higher temperatures with increasing magnetic field. The experimental data have been analyzed in the framework of a model in which we assume that the ground states of europium ions are split even without an external magnetic field. We present arguments which support this assumption and we show that it is possible to find a physical mechanism leading to the splitting which can explain the experimental results.

PACS numbers: 71.70.Ch, 75.40.Cx

## I. INTRODUCTION

Semimagnetic semiconductors (SMSs), also known as diluted magnetic semiconductors (DMS), have been studied extensively during the past two decades. Recently, there has been a considerable interest in these materials because of their possible applications in spintronics. Optical and magnetic measurements have shown that, in general, IV-VI SMSs with a  $3d$  element as the magnetic ion have a much weaker exchange interaction than that found in II-VI SMSs with the same magnetic ions. Also, the IV-VI SMSs with rare earths have a weaker exchange interaction than that found in the same materials with a  $3d$  element as the magnetic ion (for a review see Refs. 1,2,3,4). Electron spin resonance investigations in  $\text{SnTe}$  with Mn, Eu, and Gd have shown that the exchange interaction between free carriers and magnetic ions is roughly an order of magnitude smaller for Eu and Gd than for Mn.<sup>5</sup> The mechanism of the exchange interaction among magnetic ions in IV-VI SMSs is still not well understood.

Our previous investigations of the magnetic properties of  $\text{Pb}_{1-x}\text{Mn}_x\text{Te}$  and  $\text{Pb}_{1-x}\text{Eu}_x\text{Te}$  indicated a small ( $J/k_B < 1$  K), antiferromagnetic exchange interaction among magnetic ions.<sup>6,7,8</sup> In  $\text{Pb}_{1-x}\text{Eu}_x\text{Te}$  the absolute value of the exchange constant was about three times smaller than in  $\text{Pb}_{1-x}\text{Mn}_x\text{Te}$  and decreased with the increasing Eu-content. In Ref. 9 ter Haar *et al.* have observed magnetization steps in the high-field magnetization at millikelvin temperatures in  $\text{Pb}_{1-x}\text{Eu}_x\text{Te}$  and found exchange constant values similar to ours. By comparison with the results in II-VI SMSs we came to a conclusion, that in IV-VI SMSs the dominant exchange mechanism is the superexchange between nearest neighbors (NN). In order to develop a more complete model and to obtain parameters for the exchange interaction, we have made complementary measurements of the magnetic specific heat of  $\text{Pb}_{1-x}\text{Mn}_x\text{Te}$  and analyzed the

results together with the results of the magnetization and magnetic susceptibility measurements.<sup>10</sup> It turned out that the mechanism of the exchange interaction in  $\text{Pb}_{1-x}\text{Mn}_x\text{Te}$  may be more complex than just the NN superexchange. To explain the temperature and magnetic field dependence of the specific heat of  $\text{Pb}_{1-x}\text{Mn}_x\text{Te}$  it was necessary to take into account a splitting of the ground-energy state of single Mn-ions in  $\text{Pb}_{1-x}\text{Mn}_x\text{Te}$  and the  $p-d$  coupling between magnetic ion spins and free carriers.

In the present paper we report studies of the magnetic specific heat of  $\text{Pb}_{1-x}\text{Eu}_x\text{Te}$  crystals and compare the results with those obtained in  $\text{Pb}_{1-x}\text{Mn}_x\text{Te}$ . Some preliminary data have been recently reported.<sup>11</sup> This is a first investigation of the magnetic contribution to the specific heat in rare-earth-doped SMSs. In the following sections we present the experimental results and analysis of specific heat measurements and give a physical model for the magnetic specific heat of  $\text{Pb}_{1-x}\text{Eu}_x\text{Te}$ .

In theoretical analysis presented in Section III we argue that the experimentally observed magnetic specific heat is mainly due to single europium ions split in the disordered crystal environment. The splittings of magnetic ions caused by the crystal field are small and have been usually detected in EPR experiments. However, for europium in IV-VI semimagnetic semiconductors these splittings are large enough to be observed also in different kinds of measurements. In closely related semiconductors  $\text{Pb}_{1-x}\text{Eu}_x\text{S}$  and  $\text{Pb}_{1-x}\text{Eu}_x\text{Se}$  magnetization steps due to the splitting of single europium ions have been observed.<sup>12,13</sup> In  $\text{Pb}_{1-x}\text{Eu}_x\text{Te}$  we expect a similar effect.

There is no consensus in the literature concerning the mechanism of the ground state splitting of  $^8\text{S}$  rare earth ions in crystals. Several models were proposed and analyzed.<sup>14,15,16</sup> It seems that at present it is impossible to decide unequivocally which mechanism should be applied to a specific case. Instead, we suspect that in each case several mechanisms should be considered. There-

fore, in Section III we consider four different physical mechanisms leading to the splitting and estimate magnitudes of the resulting splittings.

The important part of the theoretical analysis is the incorporation of deformations of the  $\text{Pb}_{1-x}\text{Eu}_x\text{Te}$  crystal. These deformations are caused by the difference between Eu and Pb atoms and it turns out that even relatively small departures from octahedral symmetry may lead to splittings of the order 1 - 10 K. Therefore, they should be taken into account in analysis of magnetic specific heat measurements.

The theoretical considerations in the present paper are limited mainly to the case of the  $x=0.027$  sample. For this sample most of the magnetic ions are singles, i.e. they have no nearest magnetic neighbors. For the sample with higher concentration of Eu,  $x=0.073$ , although the theory may be applied formally, its quantitative predictions are not very reliable, because for such a high concentration a significant number of the Eu atoms is in larger, many atom clusters and the theoretical analysis of such a system is much more difficult.

## II. EXPERIMENT

We have measured the specific heat of  $\text{Pb}_{1-x}\text{Eu}_x\text{Te}$  with  $x$  values of 0.027 and 0.073. The samples of  $\text{Pb}_{1-x}\text{Eu}_x\text{Te}$  were grown by the Bridgman technique and the Eu concentration was estimated from the amounts of the components introduced into the growth chamber and measured by energy dispersive x-ray analysis (EDAX). The nominal  $x$ -values were 0.03 and 0.06 with uncertainty of about 20%. The crystals were cut in the shape of Hall bars with typical dimensions  $1.5 \times 2 \times 6 \text{ mm}^3$ . The samples were  $p$  type with carrier concentrations, from Hall measurements, of about  $1 \times 10^{18} \text{ cm}^{-3}$ . With increasing  $x$  the hole concentration decreased and the mobility increased.

Previously we have measured high-temperature magnetic susceptibility and low-temperature, high-field magnetization of  $\text{Pb}_{1-x}\text{Eu}_x\text{Te}$  with  $x$  up to 0.1.<sup>7,8</sup> By fitting the susceptibility data to the Curie-Weiss law we obtained the average Eu content in our samples ( $x_{av}$ ) and very small Curie-Weiss temperatures indicating an antiferromagnetic exchange between Eu ions,  $J/k_B = -0.38 \text{ K}$  and  $-0.27 \text{ K}$  for  $x_{av} = 0.027$  and 0.073, respectively.

The measurements of the heat capacity were performed in a cryostat using  $^3\text{He}$  and  $^4\text{He}$  systems over the temperature range 0.5 - 15 K in magnetic fields 0, 0.5, 1, and 2 T. We used the standard adiabatic heat-pulse method.<sup>17</sup> Errors in the heat capacity values were about 5%. The experimental details have been described elsewhere.<sup>10</sup>

In order to obtain the magnetic contribution to the specific heat,  $C_H$ , it was necessary to subtract the specific heat of the  $\text{Pb}_{1-x}\text{Eu}_x\text{Te}$  lattice from the measured total specific heat of  $\text{Pb}_{1-x}\text{Eu}_x\text{Te}$ . This was not a simple task. Bevolo *et al.* found that the specific heat of PbTe has an anomaly below 5 K and could not be fit-

ted with the standard expression  $C = \gamma T + \alpha T^3$ , where  $\gamma T$  and  $\alpha T^3$  are the electronic and lattice contributions, respectively.<sup>18</sup> In fact, they could not obtain a satisfactory fit to their data with an expression of the form,  $C = \gamma T + \alpha T^3 + \sum_{i=1}^n \delta_i T^{2i+3}$  unless  $n$  was at least 10. Therefore, we measured the heat capacity of our own Bridgman-grown PbTe sample in zero magnetic field and 2 T, over the temperature range from 0.5 to 15 K and found that the temperature dependence was the same for 0 and 2 T within our experimental error (as expected). In Ref. 10 we described this experiment and have shown the specific heat of PbTe vs temperature in zero magnetic field. In our preliminary paper we have shown the result of simple subtraction of the PbTe specific heat from the  $\text{Pb}_{1-x}\text{Eu}_x\text{Te}$  specific heat.<sup>11</sup> In the present paper we take into account the effect that the replacement of Pb with an atomic mass of 207.2 by Eu with an atomic mass of 151.97 leads to a decrease in heat capacity, even for small values of  $x$ . To account for this we divided the entire set of PbTe specific heat data by empirically determined factors, 1.11 for  $x=0.073$  and 1.04 for  $x=0.027$ , before subtracting from the  $\text{Pb}_{1-x}\text{Eu}_x\text{Te}$ . These factors were determined by assuming that at temperatures above 15 K, in the absence of an applied magnetic field, the magnetic contribution to the specific heat of  $\text{Pb}_{1-x}\text{Eu}_x\text{Te}$  is negligible. Therefore, this division by 1.11 (1.04) gave results for PbTe that were the same as those for  $\text{Pb}_{1-x}\text{Eu}_x\text{Te}$  at 15 K for  $x = 0.073$  (0.027). Since this is an empirical correction, we emphasize in the present work the data at temperatures below 5 K where the lattice specific heat is much smaller than the total specific heat. In the interesting region, below 2 K, the specific heat of PbTe was more than 3 orders of magnitude smaller than that of  $\text{Pb}_{1-x}\text{Eu}_x\text{Te}$ .

The magnetic specific heat data for  $\text{Pb}_{1-x}\text{Eu}_x\text{Te}$  are shown in Figs. 1 and 2. We believe that the scatter in the data represents the experimental error. For both  $x$ -values there is a broad maximum in the magnetic specific heat at about 2 K in zero magnetic field. The maximum is several times higher than that predicted by the cluster model of superexchange interaction between nearest neighbors. At higher magnetic fields the value of specific heat at the maximum increases and above 0.5 T it shifts to higher temperatures; for  $x = 0.073$  the shift is smaller than for  $x = 0.027$ . This behavior is different from that observed in  $\text{Pb}_{1-x}\text{Mn}_x\text{Te}$ <sup>10</sup> or  $\text{Sn}_{1-x}\text{Mn}_x\text{Te}$ ,<sup>19</sup> where the value of the magnetic specific heat at zero magnetic field and all higher fields was nearly the same, but the shift of the maximum with increasing magnetic field was bigger than in  $\text{Pb}_{1-x}\text{Eu}_x\text{Te}$ .

## III. THEORETICAL ANALYSIS

Before we start the analysis of magnetic specific heat (MSH) let us recall the model of the Europium atom in  $\text{Pb}_{1-x}\text{Eu}_x\text{Te}$  which describes quite well magnetization and magnetic susceptibility experimental data.<sup>8</sup>

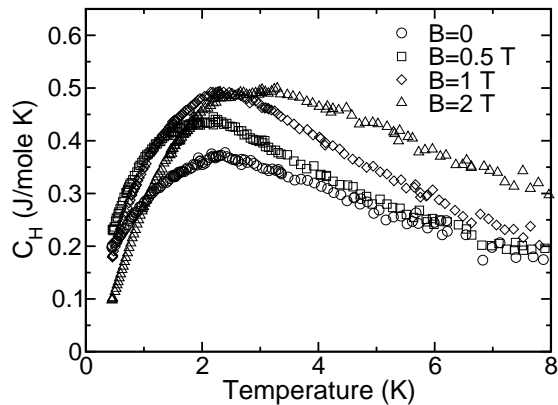


FIG. 1: Magnetic specific heat of  $\text{Pb}_{1-x}\text{Eu}_x\text{Te}$  with  $x = 0.073$  in various magnetic fields.

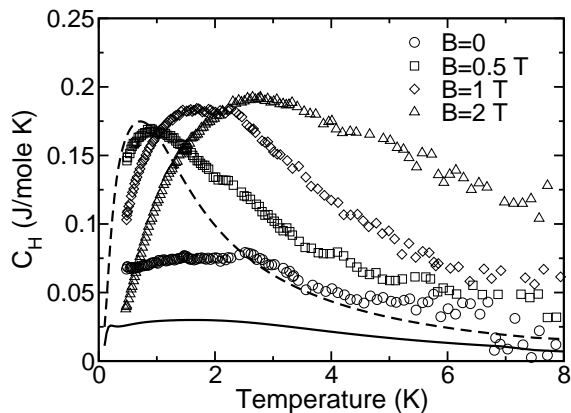


FIG. 2: Magnetic specific heat of  $\text{Pb}_{1-x}\text{Eu}_x\text{Te}$  with  $x = 0.027$  in various magnetic fields. Points - experimental data, lines - theoretical predictions of the nearest neighbours interaction model for  $B=0$  (continuous line) and  $B=0.5$  T (broken line).

The electron configuration of a free Eu atom is  $4f^7 5s^2 5p^6 6s^2$ . It is believed that when it replaces a Pb atom in PbTe the electrons from the outermost shell,  $6s^2$ , play the role of  $6p^2$  electrons of Pb and contribute to crystal bindings. Due to the strong relativistic downward shift, the energy position of  $6s^2$  Pb electrons is deeply in the valence band.<sup>20</sup> As a result we obtain  $\text{Eu}^{2+}$  ion, electrically inactive with respect to the crystal, despite the fact that it replaces Pb atom from IV group. Such a picture is confirmed by the fact that the presence of even 10% of Eu atoms has almost no effect on carrier concentration.<sup>2</sup>

According to Hund's rule the ground state of Eu ion is  $^8S$ , it means that seven  $4f$  electrons form the spin  $S=7/2$  and the total angular momentum  $L=0$ . Thus, the ground state of the ion is eightfold degenerate. This degeneracy is removed by external magnetic field,  $\mathbf{B}$  or by interaction with another magnetic ion. With such assumptions

the Hamiltonian for the spin subsystem reads

$$H = g\mu_B \sum_i \mathbf{B} \cdot \mathbf{S}_i - \sum_{ij} J_{ij} \mathbf{S}_i \cdot \mathbf{S}_j, \quad (1)$$

where the  $g$ -factor  $g = 2$ ,  $\mu_B$  is the Bohr magneton, and  $J_{ij}$  is the exchange integral between the  $i$ -th and  $j$ -th spins. If the content of Eu is small, of the order of 1-3%, we may safely assume that most of the ions have no nearest magnetic neighbors and only small percentage of them form two or three-atom clusters called, in the literature, pairs, open triangles, and closed triangles. Assuming the statistical distribution of Eu atoms in the PbTe lattice, one knows the average number of singles and the average number of atoms in pairs, open triangles, and closed triangles.<sup>21</sup> Then every thermodynamic quantity, in particular the magnetic specific heat, may be calculated.

Although such a cluster model is successful in description of magnetization in  $\text{Pb}_{1-x}\text{Eu}_x\text{Te}$ <sup>8</sup> it fails in the case of MSH. In Fig. 2 we see that the calculated MSH is much smaller than the one observed experimentally. The calculated MSH in Fig. 2, for  $B=0$  is due to pairs and triples only, because the contribution from singles, which are for  $B=0$  eight fold degenerate, is zero. The specific heat due to larger clusters has, for a sample with  $x=0.027$ , a very small contribution of about 2.5%. We also think that theories like extended nearest neighbor pair approximation (ENNPA)<sup>22</sup> based on the long range mechanism of spin - spin interaction, are not applicable to  $\text{Pb}_{1-x}\text{Eu}_x\text{Te}$  because even the nearest neighbor Eu-Eu exchange integral in  $\text{Pb}_{1-x}\text{Eu}_x\text{Te}$  is small,  $J/k_B \approx -0.25$  K<sup>8,9</sup>, and more distant interactions, which quickly decay with the distance, cannot explain the broad maximum for MSH for  $B=0$ . Let us also note, that for nonzero magnetic field the theoretical curve above 1 K lies well below the experimental points. This picture gives evidence for a non-negligible density of energy states in the energy region far above 2 K, which must be taken into account to describe the experiment properly. This density of states of the system does not result from the model described by the Hamiltonian Eq. (1).

The situation is somewhat similar to the case of  $\text{Pb}_{1-x}\text{Mn}_x\text{Te}$ , where the peak in zero magnetic field MSH is also unexpectedly high.<sup>10</sup> There is, however, at least one important difference between  $\text{Pb}_{1-x}\text{Eu}_x\text{Te}$  and  $\text{Pb}_{1-x}\text{Mn}_x\text{Te}$ . According to statistical mechanics, for any physical model describing MSH of a spin system, in particular for a model described by Eq. (1), we have following entropy relation:

$$\int_0^\infty dT \frac{C_H(T)}{T} = xR \ln(2S+1) - k_B \ln(g_H), \quad (2)$$

where  $R$  is the molar gas constant,  $S$  is the magnetic ion spin (for  $\text{Eu}^{2+}$   $S = 7/2$ ),  $C_H(T)$  is the molar magnetic specific heat at temperature  $T$  and in an external magnetic field, and  $g_H$  is the degeneracy of the ground state of the system. The degeneracy depends on the magnetic

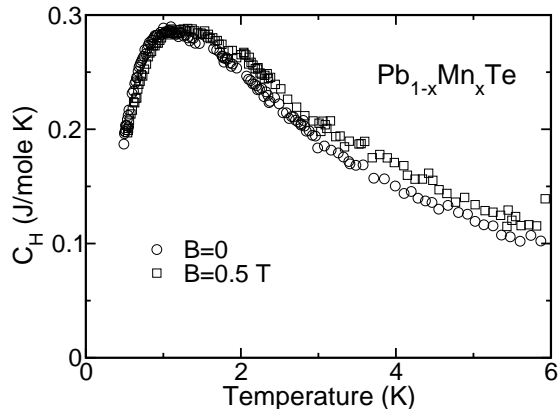


FIG. 3: Magnetic specific heat in  $\text{Pb}_{1-x}\text{Mn}_x\text{Te}$  with  $x=0.056$  in two magnetic fields (Ref. 10).

field. In an external magnetic field  $B \neq 0$ ,  $g_H=1$  and the second term on the right hand side disappears; thus calculating the difference between the left hand side of Eq. (2) for magnetic fields  $B \neq 0$  and  $B = 0$  we obtain information about the degeneracy of the ground state in zero external magnetic field. Estimations, based on experimental results presented in Ref. 10, suggest that in the case of  $\text{Pb}_{1-x}\text{Mn}_x\text{Te}$  this difference is nearly zero (see Fig. 3). Thus, in the case of  $\text{Pb}_{1-x}\text{Mn}_x\text{Te}$ , any model leading to  $g_{H=0} \neq 1$  must be rejected. This is not the case of  $\text{Pb}_{1-x}\text{Eu}_x\text{Te}$ . In Fig. 2 we see that the difference between MSH measured in  $B = 0$  and in  $B = 0.5$  T is much bigger in  $\text{Pb}_{1-x}\text{Eu}_x\text{Te}$  than in  $\text{Pb}_{1-x}\text{Mn}_x\text{Te}$ . Assuming, like in Ref. 10, the linear temperature dependence of MSH below 0.5 K we find that the value of the integral for  $B = 0.5$  T is equal to 0.41 J/mole K. For  $x=0.027$  the right hand side of Eq. (2) returns the value 0.47 J/mole K. The agreement is quite good. For  $B = 0$ , with the same assumption concerning the behavior of MSH at the lowest temperatures, the value of the integral is 0.2 J/mole K. Because the first term on the right hand side,  $xR \ln(2S + 1)$ , does not change, it means that the second one,  $k_B \ln(g_H)$ , for  $B = 0$  must be positive. Thus, the experimental data suggest that in the case of  $\text{Pb}_{1-x}\text{Eu}_x\text{Te}$  in magnetic field  $B=0$  we have non-negligible degeneracy of the ground state of the spin system. This is the important difference between  $\text{Pb}_{1-x}\text{Mn}_x\text{Te}$  and  $\text{Pb}_{1-x}\text{Eu}_x\text{Te}$ . In  $\text{Pb}_{1-x}\text{Mn}_x\text{Te}$  even in  $B=0$  the ground state is non-degenerate. The lack of degeneracy in  $\text{Pb}_{1-x}\text{Mn}_x\text{Te}$  has been discussed in Ref. 10.

At this point some clarifying remarks are necessary. First, we do *not* claim that  $\text{Pb}_{1-x}\text{Eu}_x\text{Te}$  is a system contradicting the third law of thermodynamics. In reality, if we take into account *all* interactions and system degrees of freedom, the ground state is non-degenerate. However, in our description we limit considerations to the spin subsystem and Eq. (2) is derived and may be ap-

plied only to such a subsystem. Secondly, we have no data at temperatures below 0.5 K, a region which may significantly contribute to the value of the integral. That is why the estimations of the left hand side of Eq. 2 are only semiquantitative and cannot serve as a rigorous justification of the approach introduced below. However, we think that they provide important insight into the problem and to some degree confirm the considerations given below.

In the present paper we propose that the experimentally observed MSH in zero magnetic field is due to the splitting of the energy levels of the single Eu ions. From the discussion of different aspects of splitting that are presented later, it turns out that this splitting is caused primarily by two mechanisms: the disordered crystal field potential, which leads to virtual  $4f^7 \rightarrow 4f^65d^1$  transitions, and the internal spin - orbit coupling on  $4f$  shell in the excited,  $4f^65d^1$ , state.

According to the Kramers theorem, the ground state of a single ion (of a system consisting of seven, i.e. an odd number of electrons on  $4f$  shell) is at least two-fold degenerate in the absence of an external magnetic field. Thus, the ground state of the spin subsystem, a significant part of which consists of such split noninteracting ions, is also degenerate. Such an approach is in accordance with the experimentally observed difference between the integrals, Eq. (2), for zero and nonzero magnetic fields. On the other hand, the split singles contribute to the magnetic specific heat; therefore we expect our model describing the experiment to be better than the calculated curves in Fig. 2. In the following analysis an important role is played by  $5d$  levels of europium. Let us discuss now the origin and the meaning of these states involved in the excited configuration  $4f^65d^1$  of an ion.

In the investigations of  $\text{Pb}_{1-x}\text{Eu}_x\text{Te}$  by Krenn *et al.*<sup>23</sup> the optical dipole transitions from the  $4f$  level of Eu to the vicinity of the bottom of conduction band were studied. The photon energy of these transitions for Eu concentrations corresponding to ours was found to be less than 1 eV. Notice that this kind of transition may take place only between states of different parity. Because the  $f$  functions have odd parity, the states near the bottom of the conduction band must contain states of even parity. In pure PbTe the wave functions of the bottom of the conduction band, of  $L_6^-$  symmetry, are of odd parity. Thus, to explain the existence of the optical transition we must assume that in  $\text{Pb}_{1-x}\text{Eu}_x\text{Te}$  the wave functions in the vicinity of the bottom of conduction band have certain components of even parity. The question arises about the origin of these components. The most natural candidates are  $5d$  levels of Eu. Since it is known that in EuTe the conduction band is built mainly from  $5d$  and  $6s$  states of europium,<sup>24</sup> one may expect that the addition of a few percent of Eu to PbTe will result in a contribution of  $5d$  states to the conduction band states. Of course, the presence of even parity states may be also related to the disorder introduced by addition of Eu atoms to PbTe because, strictly speaking, the group

theory considerations apply only to the perfect crystals and for  $\text{Pb}_{1-x}\text{Eu}_x\text{Te}$  containing several percent of Eu their conclusions cannot be taken too rigorously. In the approach presented below we model these states by a single, localized level of  $d$  symmetry, which we refer to as the  $5d$  level of Eu.

### A. Crystal field potential in disordered crystal

In our approach, the virtual  $4f^7 \rightarrow 4f^65d^1$  transitions are caused by the electrostatic crystal-field potential. In the present subsection we estimate the order of magnitude for this quantity in a disordered  $\text{Pb}_{1-x}\text{Eu}_x\text{Te}$  crystal.

In the crystal field theory a single  $4f$  or  $5d$  electron moves in a potential that may be expanded into the following infinite series:

$$V_{cr}(\mathbf{r}) = \sum_{l=0}^{\infty} \sum_{m=-l}^l A_{lm} \left(\frac{r}{r_0}\right)^l C_{lm}(\theta, \varphi), \quad (3)$$

where  $r_0 \approx 0.5 \text{ \AA}$  is the atomic length unit, and the functions  $C_{lm}(\theta, \varphi)$  are related to spherical harmonics  $Y_{lm}(\theta, \varphi)$  by the relation  $C_{lm}(\theta, \varphi) = \left(\frac{4\pi}{2l+1}\right)^{1/2} Y_{lm}(\theta, \varphi)$ . In our approach we use the simplest model of crystal field potential, it means we assume that the crystal field potential is due to six point charges, each of which has charge  $Ze$ , placed at  $r_i\theta_i\varphi_i$ ,  $i = 1, \dots, 6$  with respect to the europium ion. Then the coefficients  $A_{lm}$  read<sup>25</sup>

$$A_{lm} = Ze^2 \sum_{i=1}^6 \frac{r_0^l}{r_i^{l+1}} C_{lm}^*(\theta_i, \varphi_i), \quad (4)$$

where  $C_{lm}^*$  means complex conjugate to  $C_{lm}$ . In our calculations we assume that  $Z = 2$ .

Due to the difference between Eu and Pb atoms, also the Eu-Te and Pb-Te distances in  $\text{Pb}_{1-x}\text{Eu}_x\text{Te}$  are different. This difference causes local lattice deformations. These deformations are not limited to the nearest neighborhood, but extend over larger distances (several lattice constants). If the concentration of Eu atoms is very small, the average distance between Eu atoms is large. Then, although the crystal lattice is locally deformed, the symmetry of the Eu surrounding is still preserved. However, with the increasing europium content, the deformations originating from the different atoms start to overlap. Due to a random placement of Eu atoms in the lattice, we expect a random deviation of Eu-Te bond orientations from those in the perfect crystal. It turns out that these deviations cause significant ground state splittings of  $\text{Eu}^{2+}$  ions.

Let us consider a  $\text{Pb}_{1-x}\text{Eu}_x\text{Te}$  crystal with Eu content of several percent. To estimate the order of magnitude

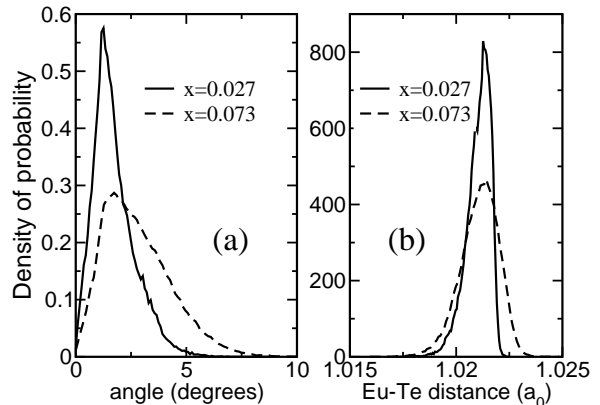


FIG. 4: (a) Distribution of bonds' deviations from the ideal crystallographic directions for two different Eu compositions. (b) Distribution of Eu-Te distances in units of lattice constant of PbTe  $a_0 = 6.46 \text{ \AA}$ .

of the bonds' deflections we performed a numerical simulation. First, we modeled a perfect lattice of crystalline PbTe containing  $50^3$  unit cells of PbTe. Next, a certain percentage of randomly chosen Pb atoms were replaced by Eu atoms. The cations were connected to anions by springs with equilibrium distances  $d_{\text{Eu-Te}} = 3.3 \text{ \AA}$  and  $d_{\text{Pb-Te}} = 3.23 \text{ \AA}$ . Due to the lack of experimental data, the bond length  $d_{\text{Eu-Te}}$  in  $\text{Pb}_{1-x}\text{Eu}_x\text{Te}$  was taken as half of EuTe lattice constant. After applying zero temperature Monte Carlo procedure, the equilibrium configuration of the lattice and the deviations of Eu-Te bonds from the perfect crystallographic directions for every Eu atom have been found. The typical bond deviation is of the order of several degrees. In Fig. 4(a) we plot the probability distribution for these deviations for two different europium contents. As it may be expected, the average deviation increases with the Eu content  $x$ . In Fig. 4(b) we plot the distribution for Eu-Te distances. As we see this distribution is very well localized around the average distance. The relative changes of the bond lengths are of the order of 0.1%.

The above, purely mechanical, model of disorder serves only to estimate the order of magnitude of deviation due to the difference between Eu-Te and Pb-Te bond lengths. It neglects, for example, the difference in strength of the bonds or the angular forces. In addition IV-VI compounds are very often disordered due to the presence of cation vacancies or granular structure of the material. Due to these reasons we expect bond deviations to be larger than estimated from Fig. 4.

In the description of our experimental data the degree of disorder will serve as one of the fitting parameters. We describe now the model of disorder which we apply to this fitting procedure.

Using a Gaussian random number generator, we generate random deviations of bond directions for each of

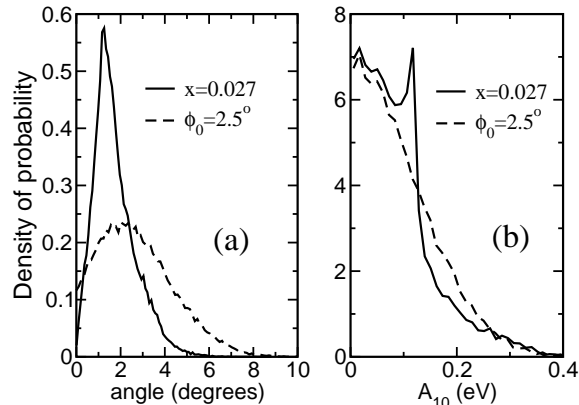


FIG. 5: Comparison of probability distributions for bond deviations (a) and crystal field potential (b). The continuous lines are the results of Monte Carlo simulations for a sample containing  $x=0.027$  of Eu and the broken lines are calculated using model of disorder described in the text for  $\phi_0=2.5^\circ$ .

the Eu atoms. More precisely, for a given Eu-Te bond, for example the one along (100) direction in the perfect crystal, we generate two random angles  $\beta$  and  $\gamma$ , both with zero mean and the standard deviation equal to  $\phi_0$ . It means that the considered bond will be characterized in spherical coordinate system by angles  $\theta = \pi/2 + \beta$  and  $\phi = \gamma$ . With slight modifications, a similar procedure is applied to the remaining five bonds of the given Eu atom. In our model of disorder we neglect changes of Eu-Te distances, because the simulations suggest that these changes are very small. For the configuration of Te atoms obtained in this way we calculate the crystal field potential, Eqs. (3, 4).

In Fig. 5 we compare the results of Monte Carlo procedure for a sample  $x=0.027$  with those resulting from the model of disorder introduced above for  $\phi_0 = 2.5^\circ$ . We see that for such value of  $\phi_0$  the differences between probability distributions for one of the crystal field coefficients,  $A_{10}$ , are not drastic.

From the above analysis we see that the presence of different cations leads to a deformation of the  $\text{Pb}_{1-x}\text{Eu}_x\text{Te}$  lattice. In particular, deformations of nearest neighbourhoods of Eu ions cause splittings of Eu ions ground states. In the next subsection we discuss physical mechanisms leading to the splittings.

## B. Mechanisms of ground state splitting of $\text{Eu}^{2+}$ ion

In this subsection we estimate the magnitudes of the ground state splitting due to different physical mechanisms.<sup>26</sup>

### 1. Direct influence of the crystal field on $4f$ electrons.

Due to the strong spin orbit coupling for  $4f$  electrons, the  $\text{Eu}^{2+}$  ion is not in a pure  $^8S$  state, but the higher energy states of the  $4f^7$  configuration are admixed<sup>14</sup> as shown:

$$|\mathcal{S}\rangle = a|^8S_{7/2}\rangle + b|^6P_{7/2}\rangle + c|^6D_{7/2}\rangle. \quad (5)$$

Thus we see that the total angular momentum  $L \neq 0$  and the ion may interact with the crystal field. The values of the coefficients  $a, b, c$  for europium may be read from Table 5.1 of Ref. 27:  $a=0.986$ ,  $b=0.167$ , and  $c=-0.011$ . For such a state, using tables of spectroscopic coefficients,<sup>28</sup> it is possible to derive matrix elements for  $\langle \mathcal{S}M | V_{cr} | \mathcal{S}M' \rangle$ .<sup>29</sup> For example, a term in Eq. (3) proportional to  $A_{20}$  yields the following term,  $H_{MM'}^{20}$  in the effective spin Hamiltonian for  $4f^7$  shell<sup>14,29</sup>

$$H_{MM'}^{20} = \delta_{MM'} \frac{2\sqrt{5}}{105} \left( M^2 - \frac{21}{4} \right) bc A_{20} \langle (r/r_0)^2 \rangle, \quad (6)$$

where  $M$  is the projection of the total spin on a quantization axis,  $M = -7/2, \dots, 7/2$ , and the average of the second power of radius for  $4f$  shell wave function for europium, in atomic units, is  $\langle (r/r_0)^2 \rangle = 0.938$  (see Ref. 30). Let us define  $\Delta$  as the energy difference between the highest and the lowest energy levels of the split ion. Then for the Hamiltonian Eq. (6),  $\Delta = (24\sqrt{5}/105)bc\langle (r/r_0)^2 \rangle A_{20}$ . From simulations we know that the average value of  $A_{20}$  is of the order of 0.01 eV. Thus  $\Delta$  is of the order of  $10^{-2}$  meV which corresponds to 0.1 K. Other terms in the expansion, Eq. (3) give splittings of the same order of magnitude or smaller. In order to explain the magnetic specific heat we need  $\Delta/k_B$  to be of the order of 1 - 10 K. Thus the mechanism based on the direct influence of the crystal field potential on  $4f$  electrons cannot explain the splitting responsible for the experimentally observed magnetic specific heat.

### 2. $4f^7 \leftrightarrow$ band states hybridization

In 1978 Barnes *et al.*<sup>15</sup> noticed that the hybridization between the  $4f$  shell and the band states leads to a splitting of the ground state of rare earth ions. The main idea of the model is to consider the excited states of the system in which the number of electrons on an ion's  $4f$  shell changes by  $\pm 1$ . According to the Hund's rule, in the excited states,  $4f^8$  and  $4f^6$ , the total angular momentum of  $4f$  electrons is nonzero. Taking into account internal spin - orbit coupling, the authors of Ref. 15 obtained an effective spin - lattice interaction leading to the ground state splitting. Let us concentrate in this Section on processes which lead to  $4f^7 \leftrightarrow 4f^6$  transitions. These processes may be important for  $\text{Pb}_{1-x}\text{Eu}_x\text{Te}$  because, according to the optical measurements performed by Krenn *et al.*<sup>23</sup>, the energy  $\epsilon_1$  necessary to transfer an electron from the  $4f$  shell to the conduction band is of the order

of 0.5 eV, which is rather small. The model has been described in Ref. 15 and has also been re-derived for the octahedral symmetry of the ion's neighborhood as discussed in Ref. 16. For completeness we describe it very briefly emphasizing the differences necessary to account for disorder in the crystal.

The ground state of the system is a Eu ion in  $4f^7$ ,  $^8S$  configuration plus the Fermi sea of electrons. This eight-fold degenerate state of the system is characterized by  $-7/2 \leq M \leq 7/2$ , where  $M$  is the projection of  $4f^7$  spin  $7/2$  on a quantization axis which we take along the (001) crystallographic direction. In the excited states we have the ion in the  $4f^6$  configuration plus one additional electron above the Fermi level, which is characterized by the set of quantum numbers  $q$ . This set of quantum numbers contains the wave vector from the first Brillouin zone, the number of the band, and the additional quantum number necessary to fully characterize the band state. This additional quantum number enumerates Kramers conjugated states. (For semiconductors, for which the band spin-orbit coupling may be neglected, i.e. spin of band carrier is a good quantum number, one may think of this additional quantum number as the projection of electron spin on a quantization axis. This is not, however, the case for  $\text{Pb}_{1-x}\text{Eu}_x\text{Te}$  where the band spin-orbit coupling cannot be neglected.) If we assume the validity of Hund's rule for the  $4f^6$  configuration,  $L=3$  and  $S=3$ , the Hamiltonian for the ion in the excited state reads:

$$H_{4f^6} = \lambda_{4f} \mathbf{L} \cdot \mathbf{S}. \quad (7)$$

The hybridization elements are:

$$\begin{aligned} \langle L_z S_z q | H | M \rangle = \\ (-1)^{L_z+1} \sum_{\sigma=\pm\frac{1}{2}} \sqrt{\frac{7/2+2\sigma M}{7}} \delta_{S_z, M-\sigma} \langle q | h | \phi_{-L_z\sigma} \rangle. \end{aligned} \quad (8)$$

The state  $|L_z S_z q\rangle$  is the excited state of the system in which the projection on the quantization axis of the total angular momentum and spin of the ion are  $L_z$  and  $S_z$ , respectively, and there is one additional electron characterized by  $q$  above the Fermi energy. The coefficient  $(-1)^{L_z+1} \sqrt{\frac{7/2+2\sigma M}{7}}$  may be derived using explicit forms of antisymmetric many electron functions for ion's states  $|L_z S_z\rangle$  and  $|M\rangle$ . The element  $\langle q | h | \phi_{-L_z\sigma} \rangle$  describes hybridization between band state  $q$  and the  $4f$  spin orbital  $\phi_{-L_z\sigma}$ . The band wave functions are calculated within the tight binding model<sup>31</sup> and the hybridization elements between  $4f$  shell and Te  $6p$  and  $6s$  orbitals are described by three constants  $V_{pf\sigma}$ ,  $V_{pf\pi}$  and  $V_{sf\sigma}$ . According to Refs. 32 and 33

$$V_{pf\sigma} = \eta_{pf\sigma} \frac{\hbar^2}{m_0} \frac{(r_p r_f^5)^{1/2}}{d^5}, \quad (9)$$

$$V_{pf\pi} = \eta_{pf\pi} \frac{\hbar^2}{m_0} \frac{(r_p r_f^5)^{1/2}}{d^5}, \quad (10)$$

where  $\eta_{pf\sigma} = 10\sqrt{21}/\pi$ ,  $\eta_{pf\pi} = -15\sqrt{7/2}/\pi$ ,  $r_p=15.9 \text{ \AA}$ ,  $r_f=0.413 \text{ \AA}$  and  $d$  is Eu-Te distance. We assume that

$V_{sf\sigma} = V_{pf\sigma}$  but the results of the calculations do not depend crucially on this assumption. The dependence of interatomic matrix elements on the direction of the Eu-Te bond with respect to the crystallographic axes of the ideal crystal is calculated according the method proposed in Ref. 34. The other details of calculations of the effective spin Hamiltonian are presented in Ref. 16.

Due to the strong localization of the  $4f$  shell, the interatomic matrix elements responsible for the  $4f$  shell band states hybridization are very small, of the order of 0.1 eV. This is the main reason that there is a small splitting  $\Delta$  despite the smallness of the transfer energy  $\epsilon_1$  which is approximately 0.5 eV. The average splitting  $\Delta/k_B$  is of the order of 0.1 K. This is again much too small a value to explain the magnetic specific heat.

### 3. $5d \leftrightarrow$ band states hybridization

Unlike the  $4f$  orbitals of the Eu ion, the  $5d$  orbitals are much more extended in space. Thus we expect the overlapping with neighboring Te orbitals to be much bigger. Recently one of the authors (A. Ł.) has proposed a new mechanism leading to the ground state splitting of rare earth ions in which the  $5d$  shell of a rare earth ion provides a bridge between the  $4f$  electrons and the rest of the crystal.<sup>16</sup> More precisely, an electron from the valence band jumps virtually onto the  $5d$  level of the rare earth ion and interacts via a Heisenberg type of exchange with the spin of the  $4f$  shell. The Hamiltonian for europium in this excited state,  $4f^7 5d^1$  is of the following form

$$H_{4f^7 5d^1} = -J_{fd} \mathbf{S} \cdot \mathbf{s} + \lambda_{5d} \mathbf{L} \cdot \mathbf{s}, \quad (11)$$

where the first term describes the exchange interaction between  $4f$  spin  $\mathbf{S}$  and the spin  $\mathbf{s}$  of the  $5d$  electron. The second term describes the spin orbit interaction on the  $5d$  shell. In the more general treatment of the problem in Ref. 16 we used two spin orbit constants. Here we use a single spin orbit constant,  $\lambda_{5d}$ , and neglect the influence of the crystal field on  $5d$  electron. For the disordered neighborhoods of europium atom which we consider in the present paper these simplifications do not change significantly the final results. Like the previous subsection the influence of the surrounding comes via the hybridization between the  $5d$  and the band states. This hybridization is described by three interatomic Eu-Te matrix elements  $V_{pd\sigma}$ ,  $V_{pd\pi}$ , and  $V_{sd\sigma}$  for which we assume following Eu-Te distance dependence<sup>8</sup>  $V_{pd\sigma} = V_{pd\sigma}^0 (a_0/d)^4$ ,  $V_{pd\pi} = V_{pd\pi}^0 (a_0/2d)^4$ , and  $V_{sd\sigma} = V_{pd\sigma}^0 (a_0/d)^{7/2}$ . Here  $a_0=6.46 \text{ \AA}$  is the lattice constant of PbTe and  $d$  is the actual Eu-Te distance along the given bond. The assumed values of three constants  $V_{pd\sigma}^0=-1.5 \text{ eV}$ ,  $V_{pd\pi}^0=0.7 \text{ eV}$  and  $V_{pd\sigma}^0=-1.6 \text{ eV}$  are close to the ones used in Ref. 35 in calculations of EuTe band structure.<sup>36</sup> The values  $J_{fd}=0.2 \text{ eV}$  and  $\lambda_{5d}=0.08 \text{ eV}$  have been taken from Table III of Ref. 37. The important parameter of the theory

is  $\epsilon_2$ , the energy necessary to transfer an electron from the top of the valence band to the  $5d$  level. Contrary to the case of gadolinium in PbTe where  $\epsilon_2$  is of the order of 0.4 eV, for europium we only know that it should be larger<sup>16</sup>. In our calculations we have assumed  $\epsilon_2=1$  eV.

For the above values of parameters the average splitting  $\Delta/k_B$  is larger than for the two previous mechanisms, of the order of 0.5 - 1 K. It remains too small, however, to explain the magnetic specific heat.

#### 4. $4f^7 \leftrightarrow 4f^6 5d^1$ transitions

The last mechanism of the splitting, which we consider, is based on  $4f^7 \leftrightarrow 4f^6 5d^1$  virtual transitions. As it has been already discussed earlier we treat  $5d$  states not as the pure atomic states but hybridized with the band states. In some sense this mechanism is complementary to the one considered in subsection 2 because in calculations in subsection 2 the  $\text{Pb}_{1-x}\text{Eu}_x\text{Te}$  band states have not contained  $5d$  orbitals. In other words, we may say that we add a certain amount of  $5d$  to the  $4f$  states.

The Hamiltonian of the model is constructed as follows. In the ground state of the ion there are seven electrons on the  $4f$  shell. The total angular momentum is zero, the total spin equals  $7/2$  and this state is eight fold degenerate. As in previous sections  $|M\rangle$  denotes a state of the ion where the projection of the total spin on a quantization axis in  $4f^7$  configuration is  $M$  ( $M = -7/2, \dots, 7/2$ ).

The excited state configuration is  $4f^6 5d^1$ . It is described by following Hamiltonian:

$$H_{4f^6 5d^1} = H_{4f^6} + \lambda_{5d} \mathbf{l} \cdot \mathbf{s} - J_{fd} \mathbf{S} \cdot \mathbf{s} + V_{cr} + \epsilon_0, \quad (12)$$

where

$$H_{4f^6} = \lambda_{4f} \mathbf{L} \cdot \mathbf{S} + \lambda_{4f}^1 (\mathbf{L} \cdot \mathbf{S})^2 \quad (13)$$

is a Hamiltonian for six electrons on  $4f$  shell describing splitting of  ${}^7F$  state due to  $4f$  spin orbit interaction. We assume that in the excited configuration, six electrons on  $4f$  shell behave according to the Hund's rule, i.e. their total spin  $S=3$  and the total angular momentum  $L = 3$ . The values of the spin orbit coupling constants  $\lambda_{4f}=0.03$  eV and  $\lambda_{4f}^1=0.0005$  eV have been fitted to describe properly a splitting of the  $4f^6$  configuration calculated from first principles (see Table VIII in Ref. 38). The second term in Eq. (12) describes spin orbit couplings on the  $5d$  shell. The next two terms correspond to exchange interactions between the  $4f$  and  $5d$  spins and the crystal field potential acting on electron on the  $5d$  shell. The last term,  $\epsilon_0$ , is the energy necessary to perform the  $4f^7 \rightarrow 4f^6 5d^1$  transition. We neglect the influence of the crystal field potential on the  $4f$  electrons since we have checked that its influence on the final result is very small.

The crystal field potential, Eq. (3), enters the Hamiltonian of the model in two places: in the term describing

the excited states, Eq. (12), and in the terms describing  $4f^7 \leftrightarrow 4f^6 5d^1$  transitions. The basis in which we describe excited states of the ion is denoted by  $|S_z L_z l_z \sigma\rangle$ , where  $S_z$  and  $L_z$  correspond to projections on a quantization axis of total spin and total angular momentum of six electrons on  $4f$  shell, respectively, while  $l_z$  and  $\sigma$  are  $z$ -th components of angular momentum and spin of the seventh, the  $5d$  electron. Using properly antisymmetrized wave functions or the concept of fractional parentage coefficients<sup>28,39</sup>, we have derived the following form for the hybridization elements:

$$\langle S_z L_z l_z \sigma | \sum_{i=1}^7 V_{cr}(\mathbf{r}_i) | M \rangle = \quad (14)$$

$$(-1)^{L_z} \sqrt{\frac{7/2+2\sigma M}{7}} \delta_{S_z, M-\sigma} \langle \phi_{l_z}^{5d} | V_{cr}(\mathbf{r}) | \phi_{-L_z}^{4f} \rangle,$$

where  $\phi_{l_z}^{5d}$  and  $\phi_{L_z}^{4f}$  are  $5d$  and  $4f$  orbitals, respectively. The external magnetic field  $B$  is taken into account by adding to the Hamiltonian Zeeman term:

$$H_B = g\mu_B B (S_z + \sigma_z) + \mu_B B (L_z + l_z), \quad (15)$$

where  $g$ -factor  $g=2$  and  $\mu_B$  is the Bohr magneton. Calculating the matrix elements of the Hamiltonian in the basis  $|M\rangle, |S_z L_z l_z \sigma\rangle$  we obtain a  $498 \times 498$  matrix. The eigenvalues of this matrix enable us to calculate the magnetic specific heat according to the standard rules of statistical mechanics. The first eight eigenvalues of the Hamiltonian matrix correspond to the split levels of the  $\text{Eu}^{2+}$  ion. The higher levels describe the  $4f^6 5d^1$  configuration and they are separated from the lowest eight ones by an energy of the order of  $\epsilon_0$ . That is why the splitting  $\Delta$  is defined here as the difference between eighth and the lowest eigenvalue. The value of the matrix element of  $r$  between radial  $4f$  and  $5d$  wave functions, necessary to calculate hybridization elements, may be estimated from the Table VI of Ref. 40. In calculations we assume that  $\langle 4f | r/r_0 | 5d \rangle = 1$ . The contribution from terms in Eq. (3) with  $l > 1$  may be omitted since the coefficients  $A_{lm}$  decay quickly with  $l$  and most important contribution comes from terms with  $l=1$ . The other parameters of the model are the same as those in the previous sections,  $J_{fd}=0.2$  eV,  $\lambda_{5d}=0.08$  eV, and  $\epsilon_0=1$  eV. For such values of parameters of the model we obtain  $\Delta/k_B$  of the order of 1-5 K.

From the analysis of different mechanisms of the splitting we conclude that the last one, i.e. the one based on  $4f^7 \leftrightarrow 4f^6 5d^1$  transitions leads to the largest ground state splitting. This mechanism, with the above values of parameters will be used to explain the magnetic specific heat for a sample containing  $x=0.027$  of europium.

### C. Magnetic specific heat

The magnetic specific heat is calculated according to standard rules of statistical mechanics. We take into account singles, pairs and triples. We assume that the Hamiltonian for pairs and triples is of the form given in

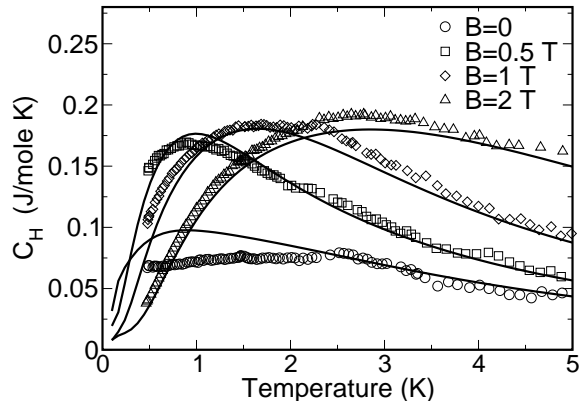


FIG. 6: Magnetic specific heat for sample  $x=0.027$ . Points - experimental results. Continuous lines - theoretical calculations for the mechanism described in Section III.B.4.

Eq. (1) with Eu-Eu exchange integral  $J/k_B=-0.25$  K.<sup>8,9</sup> For these clusters we neglect the splitting caused by the crystal field. We do not expect that the approximation would introduce a large error, because a total splitting of the pairs' energy levels in zero magnetic field is  $28 \cdot 2J$ , in our case  $28 \cdot 2 \cdot 0.25 \approx 14$  K; this is the same order of magnitude as the splitting of singles caused by the disordered crystal field. The magnetic specific heat due to singles is calculated in the following way: First we generate 100 random Eu environments as was described in Section III A. For each set of tellurium positions we calculate the energy levels of the split ion and we calculate the corresponding magnetic specific heat. As the magnetic specific heat due to singles we take the average over these 100 samples. We found that 100 samples are sufficient; for more samples we obtained nearly the same result. The parameter  $\phi_0$  is treated as the fitting parameter. The best results have been obtained for  $\phi_0=3^\circ$  and they are shown in Fig. 6.

#### D. Discussion

In the theoretical analysis of MSH we have concentrated on the sample containing  $x=0.027$  of Eu atoms. In this sample, if one assumes a random distribution of ions, more than 97% of them are in single, pair, and triple clusters and about 72% are singles. As we see from Fig. 6 the theoretical curves describe the experimental data quite well. The differences are probably due to the fact that the assumed model of disorder does not fully reflect all the complexity in a real crystal. This theoretical description has been achieved using only two fitting parameters:  $\epsilon_0$  and  $\phi_0$ . All other parameters are known from the literature.

In the sample containing  $x=0.073$  Eu, only about 40%

of ions are singles and more than 24% are in clusters containing more than three atoms. That is why the quantitative analysis is more difficult. However, the experimental results presented in Fig. 1 are in semiquantitative accordance with the proposed model.

Applying Eq. (2) for  $B \neq 0$  and for  $B = 0$  we see that the difference of the left hand sides for these two cases equals

$$\int_0^\infty dT \frac{C_{H \neq 0}(T)}{T} - \int_0^\infty dT \frac{C_{H=0}(T)}{T} = k_B \ln(g_{H=0}), \quad (16)$$

where  $g_{H=0}$  denotes the degeneracy of the ground state of the system in zero magnetic field. (As in the previous analysis the ground state of the spin system in the presence of magnetic field is nondegenerate, i.e.  $\ln(g_{H \neq 0}) = 0$ .) Calculating the integrals using experimental data with the assumptions discussed previously (temperature dependence of the specific heat for  $T < 0.5$  K is linear) we obtain this difference equal to 0.17 J/mole K. For a sample containing 0.073 of europium 40% of Eu ions are singles. It means that one mole of  $\text{Pb}_{1-x}\text{Eu}_x\text{Te}$  contains  $0.4 \cdot x \cdot N_A$  of europium singles, where  $N_A$  is the Avogadro number. Other europium ions are in larger clusters. According to our model the ground state of each Eu single is doubly degenerate. Thus the degeneracy of the ground state of the spin system due to singles is  $2^{0.4 \cdot x \cdot N_A}$  and the right hand side of Eq. (16) equals  $0.4 \cdot x \cdot R \ln 2$ . For  $x = 0.073$  we obtain 0.16 J/mole K. Assuming that the ground state of Eu ions in larger clusters is non-degenerate we obtain a very good agreement with experimental data. However, we realize that the integrals in Eq. (16) are estimated from a limited set of data. Therefore this agreement confirms our model only semiquantitatively.

The important problem we should consider is whether the proposed model is consistent with the earlier magnetization and magnetic susceptibility measurements. In the earlier theoretical description of the experimental magnetization data, using a Brillouin-function analysis for singles, we assumed that the Eu ions in zero magnetic field are not split.<sup>6,7,8</sup>

Fig. 7 shows the magnetic-field dependence of the average spin calculated with the proposed model, continuous lines, for two different temperatures. The broken lines show the behavior of Brillouin functions calculated for spin  $S=7/2$ . We see that although at the lowest temperatures the differences are noticeable, they are small. Thus our analysis has shown that the magnetic specific heat measurements reveal properties of the system (density of states) which are not reflected in the magnetization measurements.

#### IV. CONCLUSIONS

We have measured magnetic specific heat of  $\text{Pb}_{1-x}\text{Eu}_x\text{Te}$  for  $x=0.027$  and  $x=0.073$ . We have shown

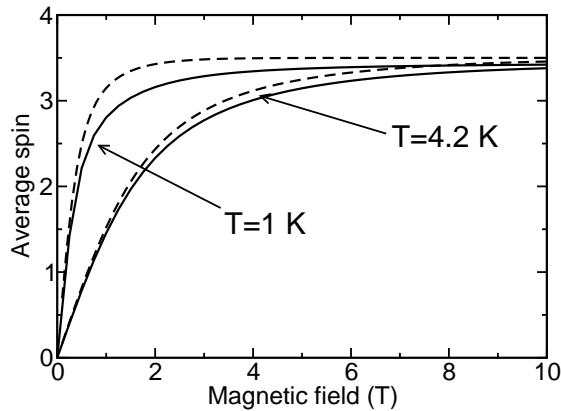


FIG. 7: Magnetic field dependence of average spin of a single ion calculated according to the model - continuous lines. The disorder is characterized by the angle  $\phi_0=3^\circ$ . For comparison, the broken lines represent plot of the Brillouin function for spin  $S=7/2$ .

that the experimental results may be explained assuming that the single Eu ions are split in a disordered crystal field potential even without external magnetic field. Analyzing the possible mechanisms of the splitting we have concluded that the main contribution to the splitting comes from the virtual  $4f^7 \leftrightarrow 4f^65d^1$  transitions. We have also shown that the model is suitable for description of the earlier measurements of magnetization.

### Acknowledgments

We are indebted to Prof. T. Story for helpful discussion. This work was supported in part by the University of Maryland Center for Superconductivity Research and by the Polish Grant PBZ-KBN-044/P03/2001.

- 
- \* Present address: Department of Physics, University of Illinois, Urbana, Illinois 61801
- <sup>1</sup> W. Dobrowolski, J. Kossut, and T. Story, in *Handbook of Magnetic Materials*, edited by K. H. J. Buschow (Elsevier, Amsterdam, 2003), vol. 15, p. 289.
  - <sup>2</sup> T. Story, in *Lead Chalcogenides: Physics and Applications*, edited by D. Khokhlov (Taylor & Francis, New York, 2003), p. 385.
  - <sup>3</sup> J. Furdyna and J. Kossut, in *Semiconductors and Semimetals* (Academic Press, New York, 1988), vol. 25.
  - <sup>4</sup> W. J. M. de Jonge and H. J. M. Swagten, *J. Magn. Magn. Mater.* **100**, 322 (1995).
  - <sup>5</sup> P. Urban and G. Sperlich, *Solid State Commun* **16**, 927 (1975).
  - <sup>6</sup> M. Górska and J. R. Anderson, *Phys. Rev. B* **38**, 9120 (1988).
  - <sup>7</sup> M. Górska, J. R. Anderson, G. Kido, and Z. Gołacki, *Solid State Commun* **75**, 363 (1990).
  - <sup>8</sup> M. Górska, J. R. Anderson, J. L. Peng, Y. Oka, J. Y-Jen, I. Mogi, D. Ravot, and Z. Gołacki, *Phys. Rev. B* **55**, 4400 (1997).
  - <sup>9</sup> E. ter Haar, V. Bindilatti, N. F. Oliveira, Jr., G. H. McCabe, Y. Shapira, Z. Gołacki, S. Charar, M. Averous, and E. J. McNiff, Jr., *Phys. Rev. B* **56**, 8912 (1997).
  - <sup>10</sup> A. Łusakowski, A. Jędrzejczak, M. Górska, V. Osinny, M. Arciszewska, W. Dobrowolski, V. Domukhovskii, B. Witkowska, T. Story, and R. R. Gałazka, *Phys. Rev. B* **65**, 165206 (2002).
  - <sup>11</sup> M. Górska, A. Łusakowski, A. Jędrzejczak, Z. Gołacki, J. R. Anderson, and H. Balci, *Acta Phys. Polon* **105**, 631 (2004).
  - <sup>12</sup> V. Bindilatti, E. ter Haar, N. F. Oliveira, Jr., M. T. Liu, Y. Shapira, X. Gratens, S. Charar, S. Isber, P. Masri, M. Averous, et al., *Phys. Rev. B* **57**, 7854 (1998).
  - <sup>13</sup> V. Bindilatti, N. F. Oliveira, Jr., Y. Shapira, G. H. McCabe, M. T. Liu, S. Isber, S. Charar, M. Averous, E. J. McNiff, Jr., and Z. Gołacki, *Phys. Rev. B* **53**, 5472 (1996).
  - <sup>14</sup> B. G. Wybourne, *Phys. Rev.* **148**, 317 (1966).
  - <sup>15</sup> S. E. Barnes, K. Baberschke, and M. Hardiman, *Phys. Rev. B* **18**, 2409 (1978).
  - <sup>16</sup> A. Łusakowski, *Phys. Rev. B* **72**, 094429 (2005).
  - <sup>17</sup> F. Morin and J. Maita, *Phys. Rev.* **129**, 1115 (1963).
  - <sup>18</sup> A. J. Bevelo, H. R. Shanks, and D. E. Eckels, *Phys. Rev. B* **13**, 3523 (1976).
  - <sup>19</sup> P. Eggenkamp, Ph.D. thesis, Eindhoven University of Technology (1994).
  - <sup>20</sup> T. Dietl, C. Śliwa, G. Bauer, and H. Pascher, *Phys. Rev. B* **49**, R2230 (1994).
  - <sup>21</sup> R. E. Behringer, *J. Chem. Phys.* **29**, 537 (1958).
  - <sup>22</sup> A. Twardowski, H. J. M. Swagten, W. J. M. de Jonge, and M. Demianiuk, *Phys. Rev. B* **36**, 7013 (1987).
  - <sup>23</sup> H. Krenn, W. Herbst, H. Pascher, Y. Ueta, G. Springholz, and G. Bauer, *Phys. Rev. B* **60**, 8117 (1999).
  - <sup>24</sup> P. Wachter, in *Handbook on the Physics and Chemistry of rare Earths*, edited by J. K. A. Gschneidner and L. Eyring (North-Holland, Amsterdam, 1979).
  - <sup>25</sup> S. Sugano, Y. Tanabe, and H. Kanimura, *Multiplets of Transition-Metal Ions in Crystals* (Academic Press New York and London, 1970).
  - <sup>26</sup> Notice the different meanings of the symbol  $\epsilon_0$  in subsections 2, 3 and 4. It always denotes energy of electron transfer, but the initial and final states in each subsection are different.
  - <sup>27</sup> D. J. Newman and W. Urban, *Adv. Phys.* **24**, 793 (1975).
  - <sup>28</sup> C. W. Nielson and G. F. Koster, *Spectroscopic Coefficients for the  $p^n$ ,  $d^n$ , and  $f^n$  Configurations* (The M. I. T. Press, Massachusetts Institute of Technology, Cambridge, Massachusetts, 1963).
  - <sup>29</sup> H. F. Brito and G. K. Liu, *J. Chem. Phys.* **112**, 4334 (2000).
  - <sup>30</sup> A. J. Freeman and R. E. Watson, *Phys. Rev.* **127**, 2058 (1962).
  - <sup>31</sup> M. Kriechbaum, P. Kocevar, H. Pascher, and G. Bauer,

- IEEE Journal of Quantum Electronics **24**, 1727 (1988).
- <sup>32</sup> W. A. Harrison and G. K. Straub, Phys. Rev. B **36**, 2695 (1987).
- <sup>33</sup> G. K. Straub and W. A. Harrison, Phys. Rev. B **31**, 7668 (1985).
- <sup>34</sup> R. R. Sharma, Phys. Rev. B **19**, 2813 (1979).
- <sup>35</sup> J. Blinowski and P. Kacman, Phys. Rev. B **64**, 045302 (2001).
- <sup>36</sup> P. Kacman, private communication.
- <sup>37</sup> T. Kasuya and A. Yanase, Rev. Mod. Phys. **40**, 684 (1968).
- <sup>38</sup> O. Visser, L. Visscher, P. J. C. Aerts, and W. C. Nieuwpoort, J. Chem. Phys. **96**, 2910 (1992).
- <sup>39</sup> B. R. Judd, *Operator techniques in atomic spectroscopy* (McGraw-Hill Book Company, Inc., 1963).
- <sup>40</sup> B. R. Judd, Phys. Rev. **127**, 750 (1962).